

## Analyses of LiNbO<sub>3</sub> wafer surface etched by ECR plasma of CHF<sub>3</sub> & CF<sub>4</sub>

Naoki Mitsugi, Kaori Shima, Masumi Ishizuka and Hirotohi Nagata

New Technology Research Laboratories, Sumitomo Osaka Cement Co., Ltd.,  
585 Toyotomi-cho, Funabashi-shi, Chiba 274-8601 Japan

LiNbO<sub>3</sub> (LN) based optical waveguide device are commonly used in optical fiber communication system as an external optical intensity modulator and an optical polarization scrambler. Recently, in order to realize LN modulators faster than 40Gb/s, the distribution of the electric field applied to the device must be adjusted to concentrate on the waveguides by machining the LN surface. In this regard, ridge-shaped optical waveguides are promising structure, and electron cyclotron resonance plasma etching of the LN surface with fluorocarbons have been attempted. Here, some unclarified phenomena occurring at the LN surface during the etching were discussed.

### 1. INTRODUCTION

A high speed external optical modulator and an optical polarization scrambler made of LiNbO<sub>3</sub> (LN) substrate have been evaluated for use in optical communication systems. For instance, an electron cyclotron resonance (ECR) plasma of fluorocarbons is considered to be suitable for etching the LN substrate because of its high chemical reactivity (1). Noguchi et al. reported high-speed LN optical modulators prepared by the ECR etching to have 3 - 4  $\mu\text{m}$  deep trenches on both sides of the optical waveguide (2 - 8). However, a problem in the dry etching process of the LN substrates has not been clarified yet. For instance, generation of LiF precipitates on the etched surface, as recently reported by us, causes a peeling of a SiO<sub>2</sub> layer on the LN surface (9, 10). The purpose of this report is to investigate and clarify such problems occurring in the fabrication of high-speed LN modulators with ridge waveguides.

### 2. EXPERIMENTAL PROCEDURES

The dry etching of the LN substrates was carried out using a commercial ECR etcher, ANELVA model L-310R, with CF<sub>4</sub> or CHF<sub>3</sub> as an etching gas. A z-cut LN wafer having 3 in. diam and 0.5mm thickness was placed on a SiC substrate holder which

faced the plasma chamber. A distance between the substrate and the acceleration electrode for the plasma outlet was about 20cm. After the etching chamber was evacuated to under  $4 \times 10^{-4}$  Pa, etching gas was introduced at a rate of 3 sccm and the pressure was kept at about  $1 \sim 4 \times 10^{-2}$  Pa. An electric power supplied to the microwave generator was 400W, and a magnet voltage and an ion acceleration voltage were set to 80 and 500V, respectively. During the etching, the substrate holder was water-cooled at 21 °C and rotated (17rpm). Under these etching conditions, typical etching rates of 800 nm/h by CF<sub>4</sub> and 700 nm/h by CHF<sub>3</sub> were obtained for the LN. The deviation in etched depth for a 3 in. diam substrate was  $\pm 20$  nm for 240 nm deep etching by CHF<sub>3</sub> for instance.

Patterned etching of the LN for fabrication of ridge waveguides was performed using a Ni film mask. The etching rate ratio of the LN to the Ni film was measured at about 3.7 independent of the etching gas. The Ni film mask was prepared on the LN substrate by conventional photolithography and an electroplated 3  $\mu\text{m}$  thick Ni film. After ECR etching, the remaining Ni was easily removed using dilute HNO<sub>3</sub> at room temperature.

### 3. RESULTS AND DISCUSSION

#### 3.1. Formation of ridge waveguides

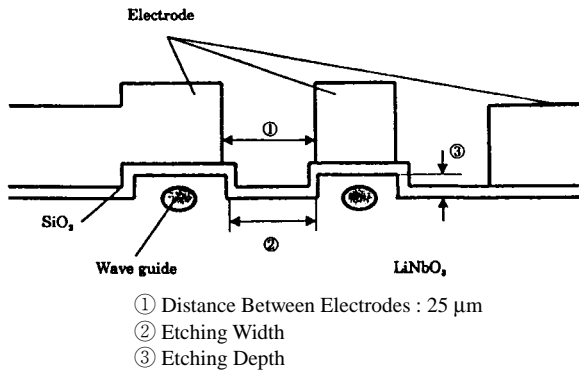


Fig.1 (a) Schematic illustration of cross section of the fabricated LN MZ optical intensity modulator having ridge waveguides.

Figure 1 shows a schematic illustration of the ridge waveguides fabricated on the z-cut LN substrate. After the Mach-Zehnder (MZ) type waveguides were formed on the substrate by a conventional Ti-diffusion technique, on both side of the MZ waveguide arms, the rectangular spaces were etched to 2.8 ~ 3.6  $\mu\text{m}$  in depth, 40  $\mu\text{m}$  in length along the waveguide and 5 or 15  $\mu\text{m}$  in width. The etched width corresponds to the gap between the obtained ridge waveguides in Fig. 1. Then, a 1.2  $\mu\text{m}$   $\text{SiO}_2$  buffer layer was deposited by rf sputtering of a  $\text{SiO}_2$  target with an  $\text{Ar}/\text{O}_2$  mixture to a thickness, and a 100 nm thick Si layer was further sputter deposited. Over the ridge waveguides covered by the  $\text{SiO}_2$  and Si layers, 17  $\mu\text{m}$  thick coplanar gold electrodes were formed by electroplating to give a 25  $\mu\text{m}$  gap between the hot and ground electrodes.

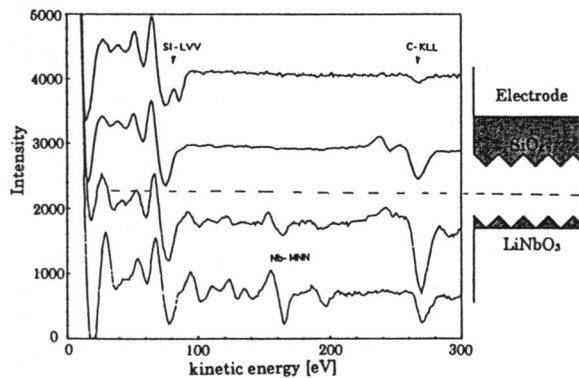


Fig. 2. Result of AES analysis for the failed device, in which the surface electrodes and the  $\text{SiO}_2$  buffer layer peeled off from the etched LN wafer surface.

#### 3.2. Problems during the etching process

In the above described, fabrication process of LN modulators with ridge waveguides, some problems occurred and discussed. Those problems were classified into two types, chemical and mechanical problems.

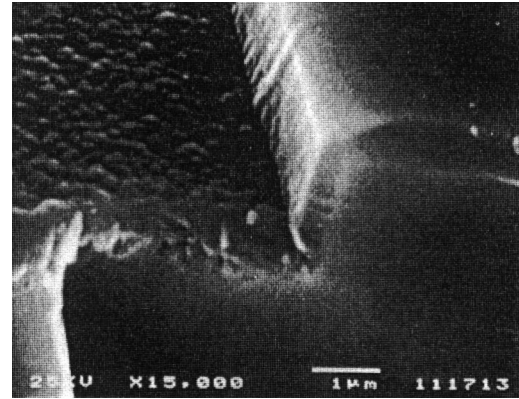


Fig.3. SEM image of the cross-section of the LN wafer with ridge waveguides and the buffer layer. The ridge waveguides were prepared by ECR etching using  $\text{CF}_4$ .

The thick ground electrodes were peeled off during the cutting process of the LN chips from the wafer. The ground electrodes were formed over the ECR etched LN surface via the  $\text{SiO}_2$  buffer layer. In our experience on thousands of conventional LN modulators made without the ECR etching process, such failure has rarely been observed. Figure 2 shows the AES profiles for surfaces of the peeled electrode and the substrate. The dashed line in the figure denotes the peeled position, and the profiles over and under the dashed line denote the peeled electrode underneath and the remaining substrate surface, respectively. The other two profiles were measured after a few minutes of Ar ion etching of the corresponding surface to exclude the effect of surface contamination. As is seen, the Auger electron peaks come from Nb were detected only from the substrate, indicating that the electrode peeled off at the boundary of the LN and the  $\text{SiO}_2$  buffer layer. In other words, the adhesive strength between the ECR etched LN and the  $\text{SiO}_2$  was weak the chemically induced problem.

Figure 3 shows a SEM image of a cross section of the ridge waveguide with only the 1.2  $\mu\text{m}$  thick  $\text{SiO}_2$  buffer layer without the electrodes. The boundary between the buffer layer and the LN ridge waveguide

was smooth and the buffer layer and waveguides adhered closely to each other. However, the boundary on the etched LN surface was rough accompanied with small voids, suggesting the inferior adhesion of the buffer layer.

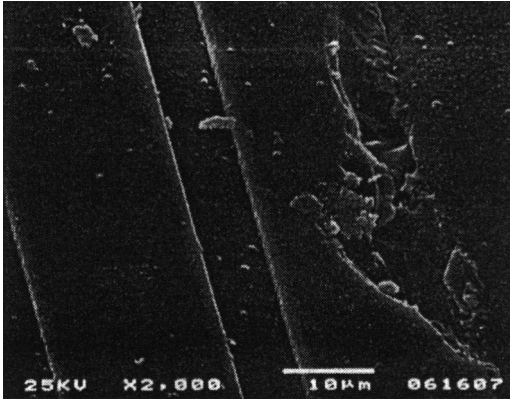


Fig. 4. SEM images of the broken ridge waveguides after the SiO<sub>2</sub> buffer layer deposition process.

In addition to the chemical problems, catastrophic mechanical problem occurred in the fabrication of the ridge waveguide devices. Figure 4 shows the SEM image for the mechanically broken ridges, in which the waveguide was also broken and could not transfer any optical signal. Such failure was found frequently after the buffer layer deposition on the substrates ECR etched by CF<sub>4</sub>. With increasing the buffer layer thickness, the number of broken waveguides increased and the fabrication yield for the devices deteriorated significantly (almost all device chips in the wafer failed due to the break at somewhere in the waveguides).

As a reason for the damaged ridge waveguides, surface stress due to the buffer layer formation was considered. Internal stress of the sputtering-deposited SiO<sub>2</sub> buffer layer on the LN was previously found to be compressive stress and tensile stress for LN surface. On the other hand, growth of a notch line along the ridge waveguides, as shown in Fig. 5, was found for the samples ECR etched by CF<sub>4</sub>. The SEM image of Fig. 5 (a) was observed before the buffer layer deposition. There was possibility that the notches were the origin of the fractured ridge waveguides with the tensile stress on the LN surface being induced by the buffer layer deposition.

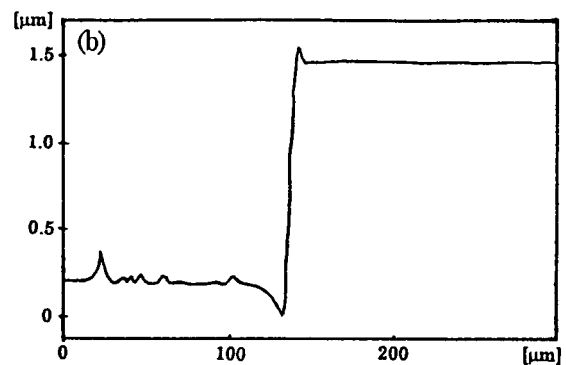
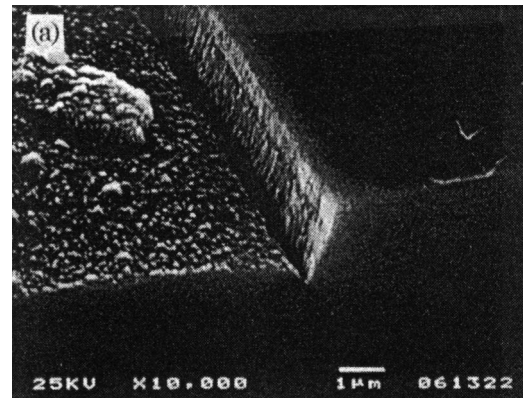


Fig. 5. (a) cross-sectional SEM image of the ridge waveguide prepared by the CF<sub>4</sub> ECR plasma etching, and (b) the corresponding surface profile measured by the stylus method.

### 3.3. Solution of problems

Results of the AES examination of the ECR etched surface, as shown in Figs. 6 (a) for the virgin LN surface and 6 (b) for the etched surface, show significant amounts of fluorine and carbon from the ECR etched surface. These contaminants are thought to deteriorate the adhesive strength of the buffer layer on the etched LN surface. The origin for the contaminants was previously investigated and found to be precipitation of LiF and polymers, possibly due to the etching gases, CHF<sub>3</sub> and CF<sub>4</sub> (9, 10).

In order to improve buffer layer adhesion, a method to remove surface contaminants was investigated. Three kind of method were attempted here; ① wet etching by dilute HNO<sub>3</sub>, ② O<sub>2</sub> annealing at 600 °C for 1 h, ③ O<sub>2</sub> plasma ashing. After the treatments, the surface of samples was evaluated by AES. Fig. 7 (a) and 7 (b) show the amount of F and C measured

for etched surface. Data of F and C were normalized by Nb peak intensity measured at same samples. As the result, F and C were easily removed by wet etching by dilute  $\text{HNO}_3$  or  $\text{O}_2$  annealing.

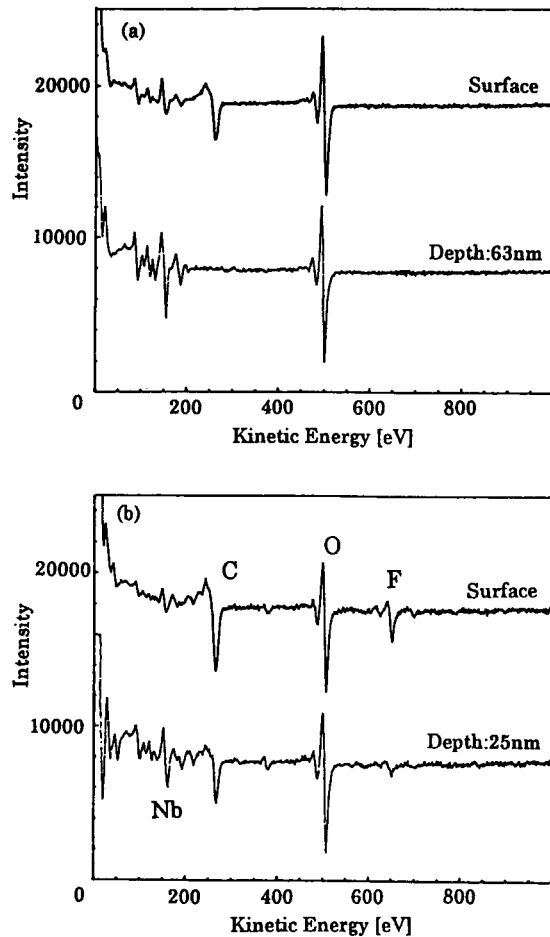


Fig. 6. AES measurement results for (a) virgin LN surface and for (b) the ECR etched surface with  $\text{CF}_4$ .

The ridge waveguide devices were prepared again, adopting process for removing the surface precipitates (especially the  $\text{LiF}$ ) before the buffer layer deposition process. The above described  $\text{O}_2$  annealing at  $600^\circ\text{C}$  and the alternative  $\text{HNO}_3$  etching were attempted. The adhesive strength of the buffer layer was improved and both buffer layer and electrodes were not peeled off, even after machining the wafer.

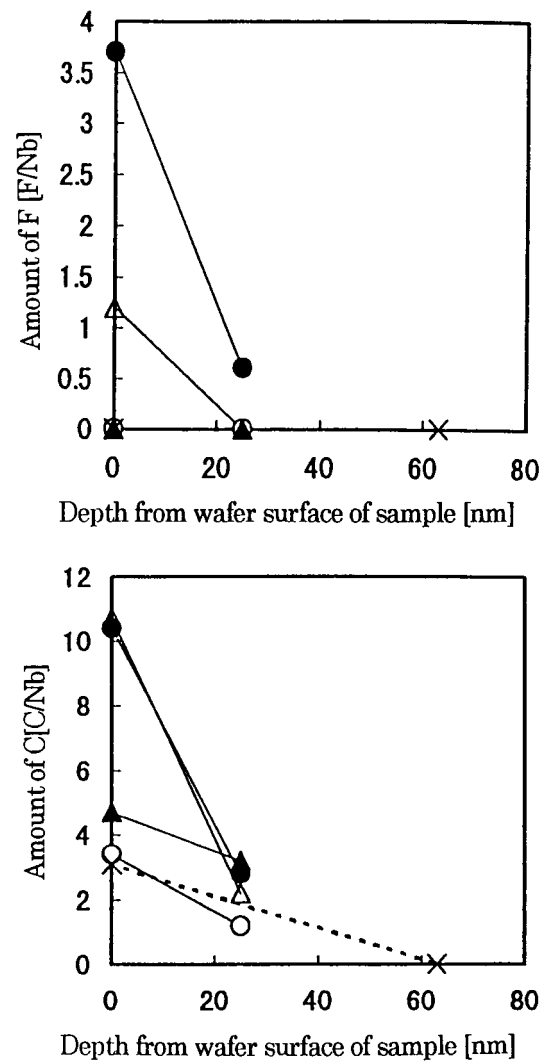


Fig. 7. Data of AES. (a) Amount of F measured on surface of samples. (b) Amount of C measured on surface of samples. (●) : after ECR etching, (○) : after wet etching by dilute  $\text{HNO}_3$ , (▲) : after  $\text{O}_2$  annealing, (△) : after  $\text{O}_2$  ashing, (×) : virgin surface)

Another problem was notches along the ridge waveguide foot formed during the dry etching (see Fig.5). This problem was found to be improved by changing the etching gas from  $\text{CF}_4$  to  $\text{CHF}_3$ , although the reason for the improvement is not known at this time. Figures 8(a) and 8(b) show the SEM image and the surface profile, respectively, of the ECR etched ridge waveguides using  $\text{CHF}_3$ . The ridges with 4 - 5  $\mu\text{m}$  height were successfully fabricated over the 3 in. diam LN wafer without any notches.

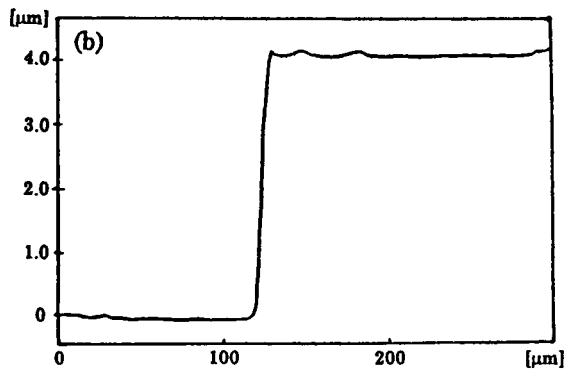
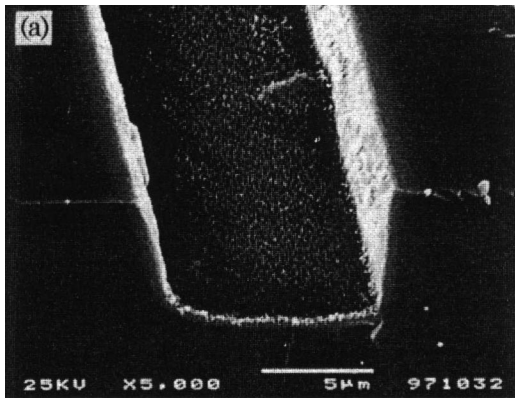


Fig. 8. (a) Cross-sectional SEM image of ridge waveguides prepared by the  $\text{CHF}_3$  ECR plasma etching, and (b) the corresponding surface profile measured by the stylus method.

### Reference

- (1) J.L. Jackel, R.E. Howard, E.L. Hu and S.P. Lyman, *Appl. Phys. Lett.* 38 (1981) 907
- (2) K.Noguchi, O.Mitomi, H.Miyazawa, and S.Seki, *J.Lightwave Technol.* 13, 1164 (1995)
- (3) K.Noguchi, O.Mitomi, and H.Miyazawa, *Optical fiber communication, OFC '96 Technical Digest* (Optical Society of America, Washington D.C.,1996) p.205.
- (4) K.Noguchi, O.Mitomi, K.Kawano, and M.Yanagibashi, *IEEE Photonics Technol. Lett.* 5,

- 52 (1993)
- (5) F. Lanrell, J. Webjo, G. Arvidsson, and J. Holmberg, *J. Lightwave Technol* 10, 606 (1992)
- (6) R.S. Cheng, W.L. Chen, and W.S. Wang, *IEEE Photonics Technol. Lett.* 7, 1282 (1995)
- (7) S.Miyazawa, *J.Appl. Phys.* 50, 4599 (1979)
- (8) C.Q.Xu, H.Okayama, and M.Kawahara, *Appl. Phys. Lett.* 64, 2504 (1994)
- (9) K.Shima, N.Mitsugi, and H.Nagata, *J.Mater. Res* 13, 527 (1998)
- (10)H.Nagata, N.Mitsugi, KShima, M.Tamai, and R.M.Haga, *J.Cryst. Growth* 187, 573 (1998)